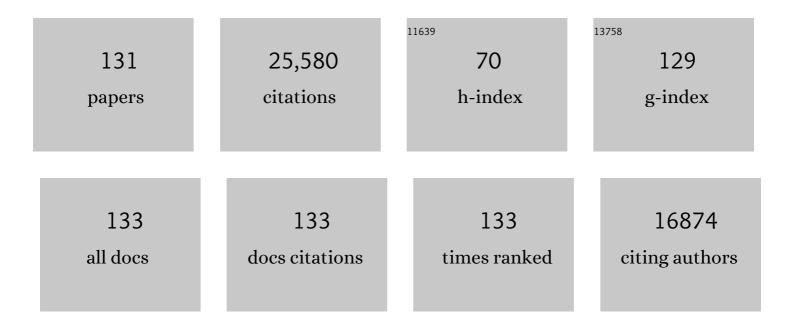
List of Publications by Year in descending order

Source: https://exaly.com/author-pdf/1849605/publications.pdf Version: 2024-02-01



#	Article	IF	CITATIONS
1	Ultrathin metal–organic framework nanosheets for electrocatalytic oxygen evolution. Nature Energy, 2016, 1, .	19.8	1,979
2	Isolated Single Iron Atoms Anchored on Nâ€Đoped Porous Carbon as an Efficient Electrocatalyst for the Oxygen Reduction Reaction. Angewandte Chemie - International Edition, 2017, 56, 6937-6941.	7.2	1,542
3	General synthesis and definitive structural identification of MN4C4 single-atom catalysts with tunable electrocatalytic activities. Nature Catalysis, 2018, 1, 63-72.	16.1	1,476
4	Atomic cobalt on nitrogen-doped graphene for hydrogen generation. Nature Communications, 2015, 6, 8668.	5.8	1,356
5	Engineering the electronic structure of single atom Ru sites via compressive strain boosts acidic water oxidation electrocatalysis. Nature Catalysis, 2019, 2, 304-313.	16.1	757
6	Defect Effects on TiO ₂ Nanosheets: Stabilizing Single Atomic Site Au and Promoting Catalytic Properties. Advanced Materials, 2018, 30, 1705369.	11.1	751
7	Enhanced oxygen reduction with single-atomic-site iron catalysts for a zinc-air battery and hydrogen-air fuel cell. Nature Communications, 2018, 9, 5422.	5.8	696
8	Structural transformation of highly active metal–organic framework electrocatalysts during the oxygen evolution reaction. Nature Energy, 2020, 5, 881-890.	19.8	647
9	Efficient Visibleâ€Lightâ€Driven Carbon Dioxide Reduction by a Singleâ€Atom Implanted Metal–Organic Framework. Angewandte Chemie - International Edition, 2016, 55, 14310-14314.	7.2	612
10	Uncoordinated Amine Groups of Metal–Organic Frameworks to Anchor Single Ru Sites as Chemoselective Catalysts toward the Hydrogenation of Quinoline. Journal of the American Chemical Society, 2017, 139, 9419-9422.	6.6	558
11	Engineering unsymmetrically coordinated Cu-S1N3 single atom sites with enhanced oxygen reduction activity. Nature Communications, 2020, 11, 3049.	5.8	537
12	Matching the kinetics of natural enzymes with a single-atom iron nanozyme. Nature Catalysis, 2021, 4, 407-417.	16.1	517
13	Dynamic traction of lattice-confined platinum atoms into mesoporous carbon matrix for hydrogen evolution reaction. Science Advances, 2018, 4, eaao6657.	4.7	460
14	lridium single-atom catalyst on nitrogen-doped carbon for formic acid oxidation synthesized using a general host–guest strategy. Nature Chemistry, 2020, 12, 764-772.	6.6	452
15	Atomicâ€Level Modulation of Electronic Density at Cobalt Singleâ€Atom Sites Derived from Metal–Organic Frameworks: Enhanced Oxygen Reduction Performance. Angewandte Chemie - International Edition, 2021, 60, 3212-3221.	7.2	445
16	Single atom electrocatalysts supported on graphene or graphene-like carbons. Chemical Society Reviews, 2019, 48, 5207-5241.	18.7	441
17	Single-Atomic Ruthenium Catalytic Sites on Nitrogen-Doped Graphene for Oxygen Reduction Reaction in Acidic Medium. ACS Nano, 2017, 11, 6930-6941.	7.3	435
18	Rational Design of Single Molybdenum Atoms Anchored on Nâ€Doped Carbon for Effective Hydrogen Evolution Reaction. Angewandte Chemie - International Edition, 2017, 56, 16086-16090.	7.2	431

#	Article	IF	CITATIONS
19	Single Tungsten Atoms Supported on MOFâ€Derived Nâ€Doped Carbon for Robust Electrochemical Hydrogen Evolution. Advanced Materials, 2018, 30, e1800396.	11.1	427
20	Single-atom Rh/N-doped carbon electrocatalyst for formic acid oxidation. Nature Nanotechnology, 2020, 15, 390-397.	15.6	420
21	Isolated Single-Atom Pd Sites in Intermetallic Nanostructures: High Catalytic Selectivity for Semihydrogenation of Alkynes. Journal of the American Chemical Society, 2017, 139, 7294-7301.	6.6	354
22	Single-atomic cobalt sites embedded in hierarchically ordered porous nitrogen-doped carbon as a superior bifunctional electrocatalyst. Proceedings of the National Academy of Sciences of the United States of America, 2018, 115, 12692-12697.	3.3	325
23	Rareâ€Earth Single Erbium Atoms for Enhanced Photocatalytic CO ₂ Reduction. Angewandte Chemie - International Edition, 2020, 59, 10651-10657.	7.2	314
24	Inâ€Situ Thermal Atomization To Convert Supported Nickel Nanoparticles into Surfaceâ€Bound Nickel Singleâ€Atom Catalysts. Angewandte Chemie - International Edition, 2018, 57, 14095-14100.	7.2	310
25	Isolated Single Iron Atoms Anchored on Nâ€Doped Porous Carbon as an Efficient Electrocatalyst for the Oxygen Reduction Reaction. Angewandte Chemie, 2017, 129, 7041-7045.	1.6	306
26	Carbon nitride supported Fe2 cluster catalysts with superior performance for alkene epoxidation. Nature Communications, 2018, 9, 2353.	5.8	278
27	Atomic interface effect of a single atom copper catalyst for enhanced oxygen reduction reactions. Energy and Environmental Science, 2019, 12, 3508-3514.	15.6	278
28	O-coordinated W-Mo dual-atom catalyst for pH-universal electrocatalytic hydrogen evolution. Science Advances, 2020, 6, eaba6586.	4.7	263
29	In Situ Phosphatizing of Triphenylphosphine Encapsulated within Metal–Organic Frameworks to Design Atomic Co ₁ –P ₁ N ₃ Interfacial Structure for Promoting Catalytic Performance. Journal of the American Chemical Society, 2020, 142, 8431-8439.	6.6	259
30	Confined Pyrolysis within Metal–Organic Frameworks To Form Uniform Ru ₃ Clusters for Efficient Oxidation of Alcohols. Journal of the American Chemical Society, 2017, 139, 9795-9798.	6.6	258
31	Metal (Hydr)oxides@Polymer Core–Shell Strategy to Metal Single-Atom Materials. Journal of the American Chemical Society, 2017, 139, 10976-10979.	6.6	257
32	Engineering Isolated Mn–N ₂ C ₂ Atomic Interface Sites for Efficient Bifunctional Oxygen Reduction and Evolution Reaction. Nano Letters, 2020, 20, 5443-5450.	4.5	249
33	Cobalt single atom site catalysts with ultrahigh metal loading for enhanced aerobic oxidation of ethylbenzene. Nano Research, 2021, 14, 2418-2423.	5.8	248
34	Discovery of main group single Sb–N ₄ active sites for CO ₂ electroreduction to formate with high efficiency. Energy and Environmental Science, 2020, 13, 2856-2863.	15.6	245
35	Microwaveâ€Assisted Rapid Synthesis of Grapheneâ€5upported Single Atomic Metals. Advanced Materials, 2018, 30, e1802146.	11.1	244
36	Intramolecular electronic coupling in porous iron cobalt (oxy)phosphide nanoboxes enhances the electrocatalytic activity for oxygen evolution. Energy and Environmental Science, 2019, 12, 3348-3355.	15.6	234

#	Article	IF	CITATIONS
37	Design of a Singleâ€Atom Indium ^{Î′+} –N ₄ Interface for Efficient Electroreduction of CO ₂ to Formate. Angewandte Chemie - International Edition, 2020, 59, 22465-22469.	7.2	232
38	Design of ultrathin Pt-Mo-Ni nanowire catalysts for ethanol electrooxidation. Science Advances, 2017, 3, e1603068.	4.7	224
39	Ultrasmall MoO _x Clusters as a Novel Cocatalyst for Photocatalytic Hydrogen Evolution. Advanced Materials, 2019, 31, e1804883.	11.1	222
40	Discovering Partially Charged Single-Atom Pt for Enhanced Anti-Markovnikov Alkene Hydrosilylation. Journal of the American Chemical Society, 2018, 140, 7407-7410.	6.6	218
41	A cocoon silk chemistry strategy to ultrathin N-doped carbon nanosheet with metal single-site catalysts. Nature Communications, 2018, 9, 3861.	5.8	210
42	Efficient and Robust Hydrogen Evolution: Phosphorus Nitride Imide Nanotubes as Supports for Anchoring Single Ruthenium Sites. Angewandte Chemie - International Edition, 2018, 57, 9495-9500.	7.2	205
43	Superior-Performance Aqueous Zinc-Ion Batteries Based on the <i>In Situ</i> Growth of MnO ₂ Nanosheets on V ₂ CT _X MXene. ACS Nano, 2021, 15, 2971-2983.	7.3	205
44	Recent Progress of Carbon-Supported Single-Atom Catalysts for Energy Conversion and Storage. Matter, 2020, 3, 1442-1476.	5.0	196
45	Gramâ€Scale Synthesis of Highâ€Loading Singleâ€Atomicâ€Site Fe Catalysts for Effective Epoxidation of Styrene. Advanced Materials, 2020, 32, e2000896.	11.1	181
46	Ni ^{II} Coordination to an Alâ€Based Metal–Organic Framework Made from 2â€Aminoterephthalate for Photocatalytic Overall Water Splitting. Angewandte Chemie - International Edition, 2017, 56, 3036-3040.	7.2	175
47	Efficient Visibleâ€Lightâ€Driven Carbon Dioxide Reduction by a Singleâ€Atom Implanted Metal–Organic Framework. Angewandte Chemie, 2016, 128, 14522-14526.	1.6	174
48	Thermal Atomization of Platinum Nanoparticles into Single Atoms: An Effective Strategy for Engineering High-Performance Nanozymes. Journal of the American Chemical Society, 2021, 143, 18643-18651.	6.6	174
49	Atomically Dispersed Ruthenium Species Inside Metal–Organic Frameworks: Combining the High Activity of Atomic Sites and the Molecular Sieving Effect of MOFs. Angewandte Chemie - International Edition, 2019, 58, 4271-4275.	7.2	162
50	Engineering the Coordination Sphere of Isolated Active Sites to Explore the Intrinsic Activity in Single-Atom Catalysts. Nano-Micro Letters, 2021, 13, 136.	14.4	138
51	Simultaneous oxidative and reductive reactions in one system by atomic design. Nature Catalysis, 2021, 4, 134-143.	16.1	132
52	N-Bridged Co–N–Ni: new bimetallic sites for promoting electrochemical CO ₂ reduction. Energy and Environmental Science, 2021, 14, 3019-3028.	15.6	128
53	One-Pot Pyrolysis to N-Doped Graphene with High-Density Pt Single Atomic Sites as Heterogeneous Catalyst for Alkene Hydrosilylation. ACS Catalysis, 2018, 8, 10004-10011.	5.5	121
54	Surface step decoration of isolated atom as electron pumping: Atomic-level insights into visible-light hydrogen evolution. Nano Energy, 2018, 45, 109-117.	8.2	118

#	Article	IF	CITATIONS
55	Etchingâ€Doping Sedimentation Equilibrium Strategy: Accelerating Kinetics on Hollow Rhâ€Doped CoFe‣ayered Double Hydroxides for Water Splitting. Advanced Functional Materials, 2020, 30, 2003556.	7.8	117
56	Engineering a metal–organic framework derived Mn–N ₄ –C _x S _y atomic interface for highly efficient oxygen reduction reaction. Chemical Science, 2020, 11, 5994-5999.	3.7	113
57	Singleâ€Site Au ^I Catalyst for Silane Oxidation with Water. Advanced Materials, 2018, 30, 1704720.	11.1	112
58	Scaleâ€Up Biomass Pathway to Cobalt Single‣ite Catalysts Anchored on Nâ€Doped Porous Carbon Nanobelt with Ultrahigh Surface Area. Advanced Functional Materials, 2018, 28, 1802167.	7.8	112
59	Hydrodeoxygenation of water-insoluble bio-oil to alkanes using a highly dispersed Pd–Mo catalyst. Nature Communications, 2017, 8, 591.	5.8	110
60	Two-Step Carbothermal Welding To Access Atomically Dispersed Pd ₁ on Three-Dimensional Zirconia Nanonet for Direct Indole Synthesis. Journal of the American Chemical Society, 2019, 141, 10590-10594.	6.6	108
61	Molecular Scalpel to Chemically Cleave Metal–Organic Frameworks for Induced Phase Transition. Journal of the American Chemical Society, 2021, 143, 6681-6690.	6.6	103
62	A heterogeneous iridium single-atom-site catalyst for highly regioselective carbenoid O–H bond insertion. Nature Catalysis, 2021, 4, 523-531.	16.1	103
63	Low oordinated CoNC on Oxygenated Graphene for Efficient Electrocatalytic H ₂ O ₂ Production. Advanced Functional Materials, 2022, 32, 2106886.	7.8	97
64	Revealing the Active Species for Aerobic Alcohol Oxidation by Using Uniform Supported Palladium Catalysts. Angewandte Chemie - International Edition, 2018, 57, 4642-4646.	7.2	93
65	Constructing a Graphene-Encapsulated Amorphous/Crystalline Heterophase NiFe Alloy by Microwave Thermal Shock for Boosting the Oxygen Evolution Reaction. ACS Catalysis, 2021, 11, 12284-12292.	5.5	93
66	Coordination mode engineering in stacked-nanosheet metal–organic frameworks to enhance catalytic reactivity and structural robustness. Nature Communications, 2019, 10, 2779.	5.8	89
67	Edge-hosted Fe-N3 sites on a multiscale porous carbon framework combining high intrinsic activity with efficient mass transport for oxygen reduction. Chem Catalysis, 2021, 1, 1291-1307.	2.9	86
68	Manipulation on active electronic states of metastable phase β-NiMoO4 for large current density hydrogen evolution. Nature Communications, 2021, 12, 5960.	5.8	86
69	Rational Design of Single Molybdenum Atoms Anchored on Nâ€Doped Carbon for Effective Hydrogen Evolution Reaction. Angewandte Chemie, 2017, 129, 16302-16306.	1.6	82
70	P-Doped NiMoO ₄ parallel arrays anchored on cobalt carbonate hydroxide with oxygen vacancies and mass transfer channels for supercapacitors and oxygen evolution. Journal of Materials Chemistry A, 2019, 7, 19589-19596.	5.2	79
71	Localized Ostwald Ripening Guided Dissolution/Regrowth to Ancient Chinese Coinâ€ s haped VO ₂ Nanoplates with Enhanced Mass Transfer for Zinc Ion Storage. Advanced Functional Materials, 2020, 30, 2000472.	7.8	76
72	Design of Aligned Porous Carbon Films with Singleâ€Atom Co–N–C Sites for Highâ€Currentâ€Density Hydrogen Generation. Advanced Materials, 2021, 33, e2103533.	11.1	76

#	Article	IF	CITATIONS
73	Interface engineered <i>in situ</i> anchoring of Co ₉ S ₈ nanoparticles into a multiple doped carbon matrix: highly efficient zinc–air batteries. Nanoscale, 2018, 10, 2649-2657.	2.8	66
74	Directed Biofabrication of Nanoparticles through Regulating Extracellular Electron Transfer. Journal of the American Chemical Society, 2017, 139, 12149-12152.	6.6	64
75	Molecular nitrogen promotes catalytic hydrodeoxygenation. Nature Catalysis, 2019, 2, 1078-1087.	16.1	63
76	Selective Production of Diethyl Maleate via Oxidative Cleavage of Lignin Aromatic Unit. CheM, 2019, 5, 2365-2377.	5.8	62
77	High-Loading Single-Atomic-Site Silver Catalysts with an Ag ₁ –C ₂ N ₁ Structure Showing Superior Performance for Epoxidation of Styrene. ACS Catalysis, 2021, 11, 4946-4954.	5.5	62
78	Direct Synthesis of Stable 1Tâ€MoS ₂ Doped with Ni Single Atoms for Water Splitting in Alkaline Media. Small, 2022, 18, e2107238.	5.2	58
79	Manganese deception on graphene and implications in catalysis. Carbon, 2018, 132, 623-631.	5.4	54
80	Rareâ€Earth Single Erbium Atoms for Enhanced Photocatalytic CO ₂ Reduction. Angewandte Chemie, 2020, 132, 10738-10744.	1.6	49
81	Toward a Unified Identification of Ti Location in the MFI Framework of High-Ti-Loaded TS-1: Combined EXAFS, XANES, and DFT Study. Journal of Physical Chemistry C, 2016, 120, 20114-20124.	1.5	45
82	Atomic‣evel Modulation of Electronic Density at Cobalt Singleâ€Atom Sites Derived from Metal–Organic Frameworks: Enhanced Oxygen Reduction Performance. Angewandte Chemie, 2021, 133, 3249-3258.	1.6	44
83	Inâ€Situ Thermal Atomization To Convert Supported Nickel Nanoparticles into Surfaceâ€Bound Nickel Singleâ€Atom Catalysts. Angewandte Chemie, 2018, 130, 14291-14296.	1.6	41
84	lodine-Doping-Induced Electronic Structure Tuning of Atomic Cobalt for Enhanced Hydrogen Evolution Electrocatalysis. ACS Nano, 2021, 15, 18125-18134.	7.3	40
85	Ni ^{II} Coordination to an Alâ€Based Metal–Organic Framework Made from 2â€Aminoterephthalate for Photocatalytic Overall Water Splitting. Angewandte Chemie, 2017, 129, 3082-3086.	1.6	37
86	Dynamic evolution of isolated Ru–FeP atomic interface sites for promoting the electrochemical hydrogen evolution reaction. Journal of Materials Chemistry A, 2020, 8, 22607-22612.	5.2	36
87	2D MOF induced accessible and exclusive Co single sites for an efficient <i>O</i> -silylation of alcohols with silanes. Chemical Communications, 2019, 55, 6563-6566.	2.2	34
88	Efficient and Robust Hydrogen Evolution: Phosphorus Nitride Imide Nanotubes as Supports for Anchoring Single Ruthenium Sites. Angewandte Chemie, 2018, 130, 9639-9644.	1.6	31
89	Atomically dispersed S-Fe-N4 for fast kinetics sodium-sulfur batteries via a dual function mechanism. Cell Reports Physical Science, 2021, 2, 100531.	2.8	31
90	Revealing the Active Species for Aerobic Alcohol Oxidation by Using Uniform Supported Palladium Catalysts. Angewandte Chemie, 2018, 130, 4732-4736.	1.6	29

#	Article	lF	CITATIONS
91	Design of a Singleâ€Atom Indium δ+ –N 4 Interface for Efficient Electroreduction of CO 2 to Formate. Angewandte Chemie, 2020, 132, 22651-22655.	1.6	29
92	Subnanometer iron clusters confined in a porous carbon matrix for highly efficient zinc–air batteries. Nanoscale Horizons, 2020, 5, 359-365.	4.1	27
93	Atomically Dispersed Ruthenium Species Inside Metal–Organic Frameworks: Combining the High Activity of Atomic Sites and the Molecular Sieving Effect of MOFs. Angewandte Chemie, 2019, 131, 4315-4319.	1.6	25
94	Transient Solid‣tate Laser Activation of Indium for Highâ€Performance Reduction of CO ₂ to Formate. Small, 2022, 18, e2201311.	5.2	22
95	Suppression of Bragg reflection glitches of a single-crystal diamond anvil cell by a polycapillary half-lens in high-pressure XAFS spectroscopy. Journal of Synchrotron Radiation, 2013, 20, 243-248.	1.0	20
96	Optimized MoP with Pseudo-Single-Atom Tungsten for Efficient Hydrogen Electrocatalysis. Chemistry of Materials, 2021, 33, 3639-3649.	3.2	20
97	Engineering Steam Induced Surface Oxygen Vacancy onto Ni–Fe Bimetallic Nanocomposite for CO ₂ Electroreduction. Small, 2022, 18, e2108034.	5.2	20
98	A bismuth based layer structured organic–inorganic hybrid material with enhanced photocatalytic activity. Journal of Colloid and Interface Science, 2016, 469, 231-236.	5.0	18
99	Effect of Nd/Mn substitution on the structure and magnetic properties of nano-BiFeO3. Journal of Alloys and Compounds, 2019, 786, 385-393.	2.8	17
100	Acid-stimulated bioassembly of high-performance quantum dots in <i>Escherichia coli</i> . Journal of Materials Chemistry A, 2019, 7, 18480-18487.	5.2	16
101	Single-Atom Ru on Al ₂ O ₃ for Highly Active and Selective 1,2-Dichloroethane Catalytic Degradation. ACS Applied Materials & Interfaces, 2021, 13, 53683-53690.	4.0	16
102	Identification and quantification of seleno-proteins by 2-DE-SR-XRF in selenium-enriched yeasts. Journal of Analytical Atomic Spectrometry, 2015, 30, 1408-1413.	1.6	15
103	Carbon-supported layered double hydroxide nanodots for efficient oxygen evolution: Active site identification and activity enhancement. Nano Research, 2021, 14, 3329-3336.	5.8	14
104	Nonrandomly Distributed Tungsten Vacancies and Interstitial Boron Trimers in Tungsten Tetraboride. Journal of Physical Chemistry C, 2019, 123, 29314-29323.	1.5	12
105	Pressure-induced drastic collapse of a high oxygen coordination shell in quartz-like <i>α</i> -GeO ₂ . New Journal of Physics, 2014, 16, 023022.	1.2	11
106	Bi entric view of the isostructural phase transitions in αâ€Bi ₂ Se ₃ and αâ€Bi ₂ Te ₃ . Physica Status Solidi (B): Basic Research, 2017, 254, 1700007.	0.7	11
107	Surface Molecular Encapsulation with Cyclodextrin in Promoting the Activity and Stability of Fe Singleâ€Atom Catalyst for Oxygen Reduction Reaction. Energy and Environmental Materials, 2023, 6, .	7.3	11
108	Comparative investigation of the vibrational properties of bulk 2 <i>H</i> –MoS ₂ and its exfoliated nanosheets under high pressure. Journal of Raman Spectroscopy, 2017, 48, 596-600.	1.2	10

#	Article	IF	CITATIONS
109	Controlled oxygen vacancy engineering on In ₂ O _{3â^'x} /CeO _{2â^'y} nanotubes for highly selective and efficient electrocatalytic nitrogen reduction. Inorganic Chemistry Frontiers, 2020, 7, 3609-3619.	3.0	10
110	Revisiting local structural changes in GeO ₂ glass at high pressure. Journal of Physics Condensed Matter, 2017, 29, 465401.	0.7	8
111	Structural changes in hexagonal WO3 under high pressure. Journal of Alloys and Compounds, 2019, 797, 1013-1017.	2.8	8
112	Prediction of topological nontrivial semimetals and pressure-induced Lifshitz transition in 1T′-MoS ₂ layered bulk polytypes. Nanoscale, 2020, 12, 22710-22717.	2.8	8
113	A rational design of an efficient counter electrode with the Co/Co ₁ P ₁ N ₃ atomic interface for promoting catalytic performance. Materials Chemistry Frontiers, 2021, 5, 3085-3092.	3.2	8
114	Local structural changes during the disordered substitutional alloy transition in Bi2Te3 by high-pressure XAFS. Journal of Applied Physics, 2018, 124, 065901.	1.1	7
115	Local insight into the La-induced structural phase transition in multiferroic BiFeO ₃ ceramics by x-ray absorption fine structure spectroscopy. Journal of Physics Condensed Matter, 2019, 31, 085402.	0.7	7
116	Innenrücktitelbild: Isolated Single Iron Atoms Anchored on Nâ€Doped Porous Carbon as an Efficient Electrocatalyst for the Oxygen Reduction Reaction (Angew. Chem. 24/2017). Angewandte Chemie, 2017, 129, 7107-7107.	1.6	6
117	Pressure-induced phase transitions of multiferroic BiFeO ₃ . Chinese Physics C, 2013, 37, 128001.	1.5	5
118	High-pressure, high-temperature synthesis and properties of the monoclinic phase of Y2O3. Chemical Research in Chinese Universities, 2016, 32, 545-548.	1.3	5
119	Extraordinary local structure deformation of superhard tungsten tetraboride under compression. Journal of Alloys and Compounds, 2020, 817, 152989.	2.8	5
120	Universal elastic-hardening-driven mechanical instability in α-quartz and quartz homeotypes under pressure. Scientific Reports, 2015, 5, 10810.	1.6	4
121	Pressure-induced phase transitions and structural evolution across the insulator–metal transition in bulk and nanoscale BiFeO ₃ . Journal of Physics Condensed Matter, 2019, 31, 265404.	0.7	4
122	Surface Ligand Tuning of Coordination Geometry and Pb 6s ² Electronic Pair Stereochemical Activity in MAPbBr ₃ Perovskite Nanoparticles: A Joint Experimental and Theoretical Insight. Journal of Physical Chemistry C, 2022, 126, 7500-7509.	1.5	4
123	Systemic contact dermatitis caused by acupuncture: A neglected route of allergen entry. Contact Dermatitis, 2021, 85, 102-105.	0.8	3
124	Observation of pressure induced charge density wave order and eightfold structure in bulk VSe2. Scientific Reports, 2021, 11, 18157.	1.6	3
125	Anharmonicity and local lattice distortion in strained Ge-dilute Si1â^'Ge alloy. Journal of Alloys and Compounds, 2015, 653, 117-121.	2.8	2
126	Anomalous lattice stiffening in tungsten tetraboride solid solutions with manganese under compression. Journal of Physics Condensed Matter, 2020, 32, 165702.	0.7	2

#	Article	IF	CITATIONS
127	Unusual suppression of tungsten 5d electron depletion in superhard tungsten tetraboride solid solution with chromium under compression. Journal of Physics Condensed Matter, 2022, 34, 035401.	0.7	1
128	Anomalous radial and angular strain relaxation around dilute p-, isoelectronic-, and n-type dopants in Si crystal. Physica B: Condensed Matter, 2017, 506, 198-204.	1.3	0
129	Biâ€centric view of the isostructural phase transitions in αâ€Bi ₂ Se ₃ and αâ€Bi ₂ Te ₃ (Phys. Status Solidi B 7/2017). Physica Status Solidi (B): Basic Research, 2017, 254, 1770238.	0.7	Ο
130	Applications of Field-reversal and Angle-dependent XMCD Techniques to Mn-based Diluted Magnetic Materials. Medziagotyra, 2019, 25, .	0.1	0
131	Studies on Location of Acupoints with X-ray Fluorescence Analysis Based on Synchrotron Radiation. Journal of Medical Imaging and Health Informatics, 2021, 11, 2178-2183.	0.2	0